Cross-section measurements of neutron-induced reactions on GaAs using monoenergetic beams from 7.5 to 15 MeV

R. Raut, A. S. Crowell, B. Fallin, C. R. Howell, C. Huibregtse, J. H. Kelley, T. Kawano, E. Kwan, G. Rusev, A. P. Tonchev, W. Tornow, D. J. Vieira, and J. B. Wilhelmy

Phys. Rev. C **83**, 044621 — Published 28 April 2011

DOI: 10.1103/PhysRevC.83.044621

Cross-Section Measurements of Neutron Induced Reactions on GaAs using Monoenergetic Beams from 7.5 to 15 MeV

R. Raut,[1,2] A. S. Crowell,[1,2] B. Fallin,[1,2] C. R. Howell,[1,2] C. Huibregtse,[1,2] J. H. Kelley,[3,2] T. Kawano,[4] E. Kwan,[1,2,*] G. Rusev,[1,2] A. P. Tonchev,[1,2] W. Tornow,[1,2] D. J. Vieira,[4] and J. B. Wilhelmy[4]

[1] *Department of Physics, Duke University, Durham, North Carolina 27708, USA*
[2] *Triangle Universities Nuclear Laboratory, Durham, North Carolina 27708, USA*
[3] *Department of Physics, North Carolina State University, Raleigh, North Carolina 27695, USA*
[4] *Los Alamos National Laboratory, Los Alamos, New Mexico 87545, USA*

(Dated: March 25, 2011)

Cross-section measurements for neutron induced reactions on GaAs have been carried out at twelve different neutron energies from 7.5 to 15 MeV using the activation technique. The monoenergetic neutron beams were produced via the ^{2}H$(d,n)^{3}$He reaction. GaAs samples were activated along with Au and Al monitor foils for determining the incident neutron flux. The induced activities of the reaction products were measured using high-resolution γ-ray spectroscopy. Cross-section for five reaction channels viz., ^{69}Ga$(n,2n)^{68}$Ga, ^{69}Ga$(n,p)^{69}$Zn^{m}, ^{71}Ga$(n,p)^{71}$Zn^{m}, ^{75}As$(n,2n)^{74}$As and ^{75}As$(n,p)^{75}$Ge, are reported. The results are compared with the previous measurements and available data evaluations. Statistical-model calculations, based on the Hauser-Feshbach formalism, have been carried out using the TALYS and the COH3 codes and compared with the experimental results.

PACS numbers: 24.60.Dr,25.40-h,25.45.-z,25.60.Dz

I. INTRODUCTION

GaAs is an important semiconductor with extensive application possibilities in research and industry. It is often preferred over other semiconductors in the construction of microwave frequency integrated circuits, infrared light-emitting diodes, laser diodes, solar cells and optical windows. It is also of significance in research related to the electronic transport and optoelectronic processes in semiconductor microstructures and nanostructures [1]. Exposure of GaAs to a flux of fast neutrons is expected to initiate transmutation processes within the semiconductor, leading to an increase in the impurity content and a consequent modification of the semiconductor properties. Cross-section measurements of neutron induced reactions on GaAs are thus important for the characterization of the semiconductor and how it might be affected by high neutron radiation environments. Such studies are of interest with regard to applications concerning national security and the stockpile stewardship program.

In general, such cross-section measurements are equally important for basic research. The experimental results can help to test different statistical model codes and contribute to constraining the parameter sets they use. Such studies are also expected to provide significant insight into the reaction mechanisms dominant in different energy regimes.

Neutron induced reactions on individual Ga and As isotopes have been studied for many years. Nesaraja *et al.* [2, 3] studied ^{71}Ga$(n,p)^{71}$Zn^{m} and ^{69}Ga$(n,p)^{69}$Zn^{m} reactions in the energy range from 6.2 MeV to 12.4 MeV using the activation technique. They reported cross-section values with uncertainties of 9-20%, with most of the uncertainties coming from counting statistics and the radiochemical procedures employed to isolate the activated products of interest from the matrix activity.

Birn *et al.* [4] studied the reactions ^{75}As$(n,p)^{75}$Ge, ^{75}As$(n,\alpha)^{72}$Ga and ^{75}As$(n,2n)^{74}$As in the energy range from 6.3 to 14.7 MeV and reported the cross-section values with uncertainties 10-20%. Konno *et al.* [5, 6] studied the ^{75}As$(n,p)^{75}$Ge and the ^{75}As$(n,2n)^{74}$As reactions at neutron energies from 13.3 to 14.9 MeV and reported the cross-section values with uncertainties of less than 10%. However, the measurement was restricted to closely spaced energy values only around 14 MeV. Similarly, Okumura [7] carried out cross-section measurements for the ^{75}As$(n,p)^{75}$Ge reaction from 13.4 MeV to 15.0 MeV and reported results with less than 5% uncertainty.

Pu *et al.* [8] studied the ^{69}Ga$(n,2n)$ reaction in the energy range 13.5 to 14.6 MeV with uncertainties of around 4%. But this measurement was limited to only three energies around the 14 MeV region. Bormann *et al.* [9] had studied the same reaction in 1965 over a broader energy range from 12.6 to 19.6 MeV and determined cross-sections with uncertainties of around 10%. Unlike the recent works that use high resolution γ-ray spectroscopy to measure the activated samples, Bormann *et al.* [9] used a coincidence setup of two

*Present address: Physics Division, Lawrence Livermore National Laboratory, Livermore, California 94550, USA

NaI(Tl) detectors to count the annihilation γ-rays of the positrons from the β^+-decay of the ^{68}Ga product nucleus. In fact, this was the first measurement of the excitation function for this reaction.

Apart from the works referred to already, there are other studies that will be cited in the course of this paper. However, despite continued effort for several decades, there still lacks a comprehensive measurement of the neutron induced reactions on Ga and As over a broad energy range with small uncertainties plus a detailed comparison of the measured cross sections with the results of statistical-model calculations and the latest data evaluations. The present work reports cross-section measurements on five reactions ^{69}Ga$(n,2n)^{68}$Ga, ^{69}Ga$(n,p)^{69}$Zn^m, ^{71}Ga$(n,p)^{71}$Zn^m, ^{75}As$(n,2n)^{74}$As and ^{75}As$(n,p)^{75}$Ge, over an energy range from 7.5 to 15 MeV. Monoenergetic neutron beams with high flux, pure activation samples, and high resolution γ-ray spectroscopy techniques have helped restrict the uncertainties on the measurements. The results are compared with those from statistical-model calculations based on the Hauser-Feshbach formalism, using two different codes. The cross-section values are discussed in the light of the literature data, mentioned above, and the latest cross-section data evaluations.

II. EXPERIMENTAL DETAILS

Neutron activation of GaAs foils was carried out at the 10 MV FN Tandem Accelerator at the Triangle Universities Nuclear Laboratory (TUNL). The monoenergetic neutron beam was produced via the ^{2}H$(d,n)^3$He reaction, known for its high neutron yield in the energy regime of the measurements. Deuterium gas was contained in a 3 cm long cylindrical cell, at pressure of around 3 atm. The cell was sealed from the beamline vacuum by a 0.635 mm thin Havar foil. The pressure in the gas cell and the energy losses of the deuteron beam in the Havar foil contributed to the energy spread of the neutron beam. This energy spread was calculated using the program MAGNET [10] with the incident deuteron beam energy, the length of the gas cell, the deuterium gas pressure, the thickness of the Havar foil, and the ambient temperature as inputs.

The GaAs samples were semiconductor grade wafers, chemically pure to 99.9%. They were cut into 1 cm $\times$ 1 cm targets and mounted normal to the incident beam at a distance of 2.6 cm downstream from the deuteron beam stop. Natural Al and Au foils, also cut into 1 cm $\times$ 1 cm dimensions, were mounted on either face of the GaAs samples and irradiated with them in order to determine the neutron flux incident on the samples. The schematic representation of the experimental arrangements is illustrated in Fig. 1. The large (more than 10 m) open space around the gas cell in the experimental area helped in minimizing the "room-return" neutrons. The angular distribution of the neutron flux across the width of the sample was used for estimating the energy spread of the beam. The angular distribution was calculated from the NEUYIE program of the DROSG-2000 package [11]. The type of reaction used to produce the neutron beam, the neutron energy at 0°, and the required angles for the calculations were provided as inputs to the NEUYIE program.

The GaAs samples were irradiated at twelve different neutrons energies, E_n = 7.5(2), 8.0(1), 8.5(2), 9.5(1), 10.2(1), 11.0(1), 11.5(1), 12.5(1), 13.25(10), 14.0(1), 14.5(1), and 15.0(1) MeV, where the numbers in the parentheses represent the energy spread of the neutron beam. Three sets of measurements were carried out to span this energy range. The neutron flux during each irradiation was monitored using an NE-213 liquid scintillator detector and was kept constant throughout the activation run. The neutron flux incident on the samples was about 10^7 cm^{-2}s^{-1}. At each neutron energy two separate irradiation runs were carried out, one being for a shorter (around 3 hours) duration and the other for a longer (around 15 hours) period. The short run was primarily aimed at measuring the short-lived products, with half-lives of around 1 hour, without causing any saturation in their decay. At the highest energies, 14, 14.5 and 15 MeV, only a single run of around 6 hours was carried out.

Following the irradiations, the samples were measured in the TUNL low-background counting facility using HPGe detectors. One 60% HPGe detector was used to count the GaAs samples while the Au and Al monitor foils were measured in a 20% extended range HPGe detector. The detectors were elaborately shielded against room and cosmic background radiations. The samples being measured were placed in alumunium containers and positioned at a distance of 3 cm from front face of the respective detector throughout the offline measurements.

The efficiency and the energy calibrations of the HPGe detectors were carried out with the standard radioactive sources ^{152}Eu, ^{60}Co, ^{133}Ba, and ^{137}Cs. The sources were measured in the same containers and positioned at the same distance from the detector face as the actual samples.

The data acquisition system used in the offline measurements was Canberra Multiport II MCA, supported by the GENIE 2000 software. The chosen distance between the activated samples and the detector face restricted pile-up and coincidence summing effects. Nevertheless, a pile-up rejection (PUR) circuit was implemented by connecting the PUR output of the spectroscopic amplifier to the corresponding ADC, thus

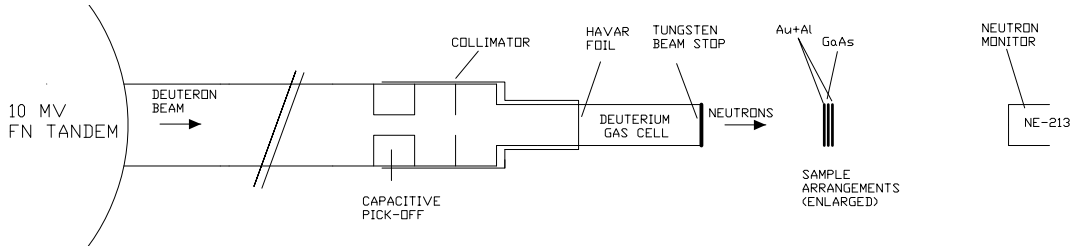

FIG. 1: Schematic representation of the experimental setup at the Neutron Time-of-Flight Area of the 10 MV FN Tandem in Triangle Universities Nuclear Laboratory.

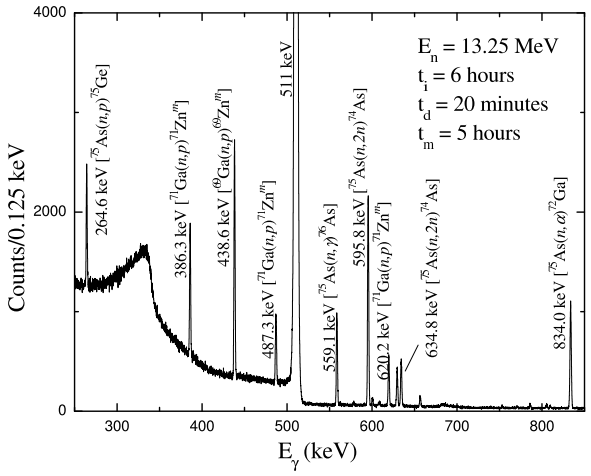

FIG. 2: Typical γ-ray spectrum from measuring the activated GaAs sample using a HPGe detector. The reaction channels and the respective gamma transition peaks are labelled.

eliminating pile-up events. However, in the present measurements, the counting rate in the HPGe detectors was low, typically $\sim$ 100-200 cps, and the fraction of the pile-up events was insignificantly small ($< 1\%$). The activated GaAs samples were counted in discrete cycles of 0.5 or 1.0 hour period, to enable tracking of the decay curve measurements of the products of interest and thus confirming their identity, as discussed in the next section.

III. DATA ANALYSIS

The acquired γ-ray spectra, from the offline measurements of the activated samples, were analyzed to identify the reaction products and to determine the respective peak areas using the software Tv [12]. A typical γ-ray spectrum from measuring an activated GaAs sample using a HPGe detector is shown in Fig. 2. In the present work, only the products with half-lives of about 1 hour or more have been studied. Table I lists the different reaction channels studied in the present measurements along with the half-lives of the products and the γ-ray transition energies used to identify them, and the corresponding branching ratios used to calculate the respective cross-sections. In addition, Table I lists the reactions associated with the Au and the Al monitor foils used for flux normalization. The half-lives of the products of interest were also estimated from the cycle measurements of the activated samples and compared with the adopted values. The calculations for some of the nuclei of interest are illustrated in Fig. 3 and are in good agreement with the established values from the National Nuclear Data Center database Nudat 2.5 [13] recorded in Table I. The branching ratios for the γ-ray transitions and the Q-values for the reaction channels of interest are quoted from the same source [13].

The cross-sections for the reaction channels of interest were calculated from the well known activation formula [14] according to which the induced activity is given by,

$$A = \sigma\phi n(1 - e^{-\lambda t_i})e^{-\lambda t_d}(1 - e^{-\lambda t_m}) \qquad (1)$$

where σ is the cross-section, ϕ is the incident flux, n is the number of target nuclei, t_i is the irradiation time, t_d is the decay time before the commencement of the offline counting, and t_m is the measurement time. The induced activity is represented by the peak area of the respective γ-ray transition normalized by the corresponding branching ratio, the disintegration rate of

TABLE I: Neutron induced reactions on GaAs and monitor foils measured in the present work.

Reaction Channel	Product Half-life	Q-value (keV)	E_γ (keV)	I_γ (%)
	GaAs Reactions			
^{69}Ga$(n,2n)^{68}$Ga	67.71(9) min	-10312.95	1077.34	3.22
^{69}Ga$(n,p)^{69}$Zn^m	13.76(2) h	-127.44	438.634	94.77(20)
^{71}Ga$(n,p)^{71}$Zn^m	3.96(5) h	-2031.0	386.28	93
^{75}As$(n,2n)^{74}$As	17.77(2) d	-10243.76	634.78	15.4(10)
^{75}As$(n,p)^{75}$Ge	82.78(4) min	-393.63	264.6	11.4
	Monitor Reactions			
^{197}Au$(n,2n)^{196}$Au	6.1669(6) d	-8072.39	355.73	0.87
^{27}Al$(n,\alpha)^{24}$Na	14.997(12) h	-3132.14	1368.626	99.9936(15)

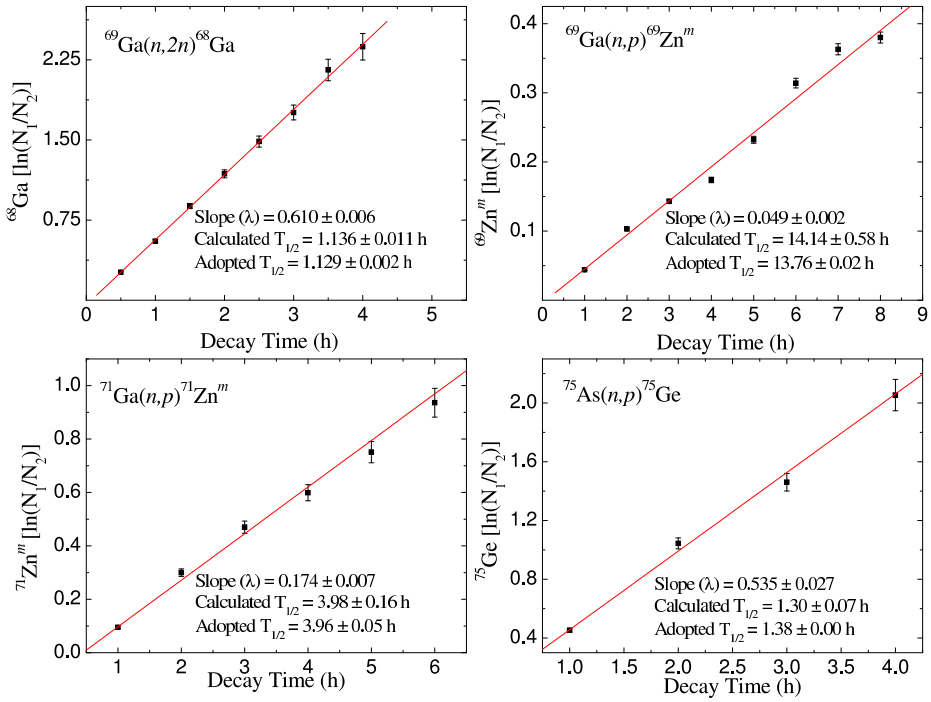

FIG. 3: Determination of half-lives for the activation products of interest. N_1 is the peak area for the first cycle of measurement while N_2 is that in each subsequent cycle. Each cycle consisted of 0.5 or 1.0 hour period. The γ-ray transitions used for different nuclei are listed in Table I.

the radioactive product, and the absolute efficiency of the detector.

One of the key ingredients in the cross-section measurements is the determination of the incident flux. The incident flux in the present measurements was obtained from the monitor reactions on the Au and Al foils irradiated with the GaAs samples. The required cross-section values for the ^{197}Au$(n,2n)$ reaction were taken from the work of Martínez-Rico [15] while those for the ^{27}Al(n,α) reaction were reported by Condé [16]. Since the threshold for the Au monitor reaction is higher than the incident neutron energy at E_n = 7.5 and 8.0 MeV, the flux at these energies was determined only from the Al monitor foil. Even at E_n = 8.5 and 9.5 MeV, though the incident neutron energy is higher than the threshold for the Au monitor reaction, the corresponding cross-sections are reported with large uncertainty and thus the flux at these energies was also obtained only from the Al monitor foil. In general it is noted that the cross-sections for the Al monitor reaction are reported with less uncertainty than those for Au, especially below

12 MeV. Thus, in calculating the flux at each energy from the average of the Au and the Al monitor foils, each was weighted according to its respective uncertainty in order to properly determine the uncertainty of the final results.

Another concern in the cross-section measurements of the neutron-induced reactions is the uncertainty associated with the presence of low energy neutrons. At neutron energies higher than 10 MeV, the ^{2}H$(d,n)^3$He reaction is known to produce low energy neutrons by the break-up of the incident or target deuteron, ^{2}H(d,np)^{2}H, in the gas cell. We have used time-of-flight measurements [17] at different neutron energies from 8 to 14 MeV in order to estimate the relative yields of the break-up and the monoenergetic neutrons. The present measurements were carried out in the same experimental setup and under the same conditions of gas cell pressure, geometry, and other important factors as in [17]. The yield distribution for the 14 MeV neutrons from the said measurements is illustrated in Fig. 4. The correction factor for the break-up neutrons was calculated from the equation [14],

$$c_{bu} = 1 - \frac{\int_0^{E^{bu}_{max}} \sigma(E)Y(E)dE}{\int_0^{E_{max}} \sigma(E)Y(E)dE} \qquad (2)$$

where $Y(E)$ is the relative yield of the neutrons with energy E and $\sigma(E)$ is the cross-section at this energy for the reaction under consideration. The quantity E^{bu}_{max} is the maximum energy of the break-up neutrons and E_{max} is the maximum energy of the neutron beam of interest, including its energy spread. The E^{bu}_{max} and E_{max} for 14 MeV neutrons is illustrated in Fig. 4. The integrals were solved numerically by interpolating the neutron spectrum and the excitation function to the same energy grid. The cross sections for the reactions of interest were taken from the statistical-model calculations using the TALYS code [18]. This was in view of the satisfactory agreement of the calculations to the experimental data, as discussed in the next section. Further, the large number of energy values used in the calculations ensures a reliable interpolation. The correction required due to interference from the low energy neutrons depends on the specific reaction, its respective threshold, and the shape of the excitation function. For the ^{197}Au$(n,2n)^{196}$Au monitor reaction, the correction required was insignificant ($\leq$ 1%) while for the ^{27}Al$(n,\alpha)^{24}$Na monitor reaction, which has a low threshold, the correction was up to 7% at 15 MeV. As far as the reactions of interest are concerned, for the ^{69}Ga$(n,2n)^{68}$Ga and the ^{75}As$(n,2n)^{74}$As reactions, with thresholds above 10 MeV, the breakup contribution was insignificantly small. For the ^{69}Ga$(n,p)^{69}$Zn^m reaction, with a very low threshold, the correction required was 9-14% at the highest energies. Similarly, for the ^{71}Ga$(n,p)^{71}$Zn^m and the ^{75}As$(n,p)^{75}$Ge reactions, the breakup contribution calculated was 5-7% at energies 14-15 MeV. It is difficult to assign the uncertainty in calculating the contribution from the low energy neutrons. The assigned uncertainty of $\leq$ 1% is from the interpolation method used to calculate the cross-section. However, our determination of the breakup contribution is based on the actual measurements of the neutron spectra and agrees with the observations of Birn *et al.* [4] for the ^{75}As$(n,p)^{75}$Ge and the ^{75}As$(n,2n)^{74}$As reactions. In the latest published results for the ^{69}Ga$(n,p)^{69}$Zn^m and ^{71}Ga$(n,p)^{71}$Zn^m reactions, Nesaraja *et al.* [2, 3] quoted only the wide range of 1-10% for the size of the correction due to break-up neutrons. This is consistent with our observations.

In addition to the break-up reaction, low energy neutrons can also originate from the break-up of the deuteron beam in the entrance window of the gas cell or the tantalum beamstop, and in other parts of the experimental structure. Measurements were carried out in ref. [17] with an empty gas cell in order to estimate the yield distribution of these neutrons. The results of these gas-out measurements are plotted in Fig. 4 for the deuteron beam energy equal to that required to produce the 14 MeV neutrons. It is observed that the yield contribution of these neutrons, resulting from the deuteron break-up in the structural materials, is insignificant even at the highest deuteron beam energies used in the present work.

The absolute efficiency of the γ-ray detector was calculated from the source measurements mentioned in the previous section. The sources and the magnitudes of the uncertainties in the present measurements are summarized in Table II.

TABLE II: Sources and approximate magnitudes (in %) of the uncertainties in the present cross-section measurements.

Uncertainty	Magnitude (%)
Statistics	1-2[a]
Sample mass	< 1
Detector efficiency	2-3
Branching ratio	≤ 1
Product half-life	≤ 1
Monitor cross-section	1-4 (Al)
	1-4 (Au)[b]
Low-energy neutrons	< 1
Total[c]	3-5

[a]For reactions at or near threshold energies, the statistical uncertainty can be as high as 7%.

[b]Below 12 MeV, the uncertainty on the Au monitor reaction is 8-12%.

[c]For specific reactions, especially near threshold, the total uncertainty is 10-11%, as detailed in III.

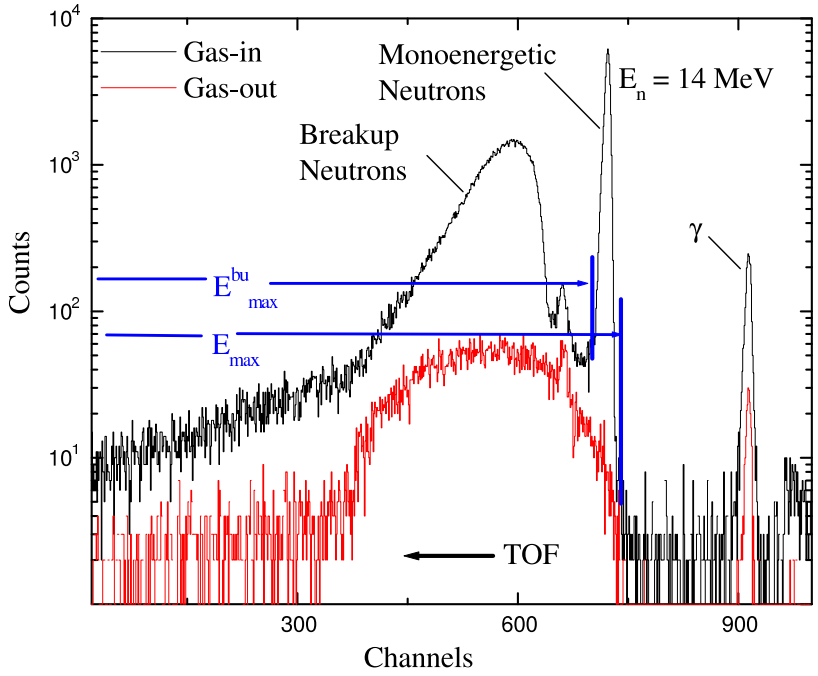

FIG. 4: (Color online). The black plot in the time-of-flight spectra (time increases from right to left) illustrates the yield distribution for the 14 MeV neutrons from the ^{2}H$(d,n)^{3}$He reaction, acquired in an identical setup as used in the present measurements. The red plot represents the yield distribution of the neutrons in a gas-out run with the same deuteron beam energy. The γ-rays originate from reactions in the Havar foil and the beam stop and have the shortest time-of-flight. The plots are not normalized to the detector efficiency.

IV. RESULTS AND DISCUSSIONS

The cross-section values for the five reactions on Ga and As at twelve different neutron energies as measured in the present work are given in the Table III. Fig. 5 shows the measured cross-sections as a function of the incident neutron energy from 7.5 to 15 MeV along with the results from statistical-model calculations, the latest evaluations, and the literature data. In this section, we first discuss the experimental results of the present work in the context of the existing literature data and available evaluations. Thereafter we describe the statistical-model calculations, first with a global parameter set and then with possible parameter adjustments.

A. Comparison with Literature Data and Evaluations

The cross-section results for the ^{69}Ga$(n,2n)^{68}$Ga reaction from the present work are consistently lower than the previously reported values by Rayburn *et al.* [19], Bormann *et al.* [9], and Pu *et al.* [8]. However, it is noteworthy to mention the different experimental techniques adopted in the previous measurements of the ^{69}Ga$(n,2n)$ cross sections, compared to the present work. The measurements of Rayburn *et al.* and Bormann *et al.*, both carried out in the 1960s before the advent of the Ge detectors, used coincidence between annihilation 511 keV γ-rays in NaI(Tl) detectors for determining the cross sections. Pu *et al.*, however, used the activation technique similar to the present work and measured the activated samples with high resolution Ge detectors. But, the monitor reaction used for flux estimation was ^{93}Nb$(n,2n)$, different from the Au and Al reactions used in the present measurements, and there is no mention of any break-up correction considered for determining the reaction cross-sections. The difference in the cross-section values might stem out from any of these factors. For the ^{69}Ga$(n,p)^{69}$Zn^{m} reaction, the measured cross-sections in the present work are in good agreement with the results of Nesaraja *et al.* [2], within the uncertainties quoted by the latter. The results from Pu *et al.* [8] at a single energy is discrepant with respect to the shape of the excitation function set by the present measurements as well as that by Nesaraja *et al.*.

As far as the ^{71}Ga$(n,p)^{71}$Zn^{m} reaction is concerned, the cross-section values from the present measurements agree with those of Nesaraja *et al.* [2], only with substantially lower uncertainties than the latter. The present measurements also agree well with the measurements of Pu *et al.* [8] and Qaim *et al.* [20] around 14 MeV while that of Vinitskaya *et al.* [21] is somewhat low, though overlapping with the present measurements within the quoted uncertainty.

TABLE III: Cross-section values for different reaction channels measured in the present work, at neutron energies from E_n = 7.5 to 15 MeV.

Neutron Energy (MeV)	Cross-Section (mb) ^{69}Ga$(n,2n)^{68}$Ga	^{69}Ga$(n,p)^{69}$Zn^m	^{71}Ga$(n,p)^{71}$Zn^m	^{75}As$(n,2n)^{74}$As	^{75}As$(n,p)^{75}$Ge
7.5±0.2		9.3±0.3	1.3±0.1		5.6±0.2
8.0±0.1		10.5±0.3	1.9±0.1		8.3±0.3
8.5±0.2		12.8±0.5	2.3±0.2		9.8±0.5
9.5±0.1		16.1±0.5	3.8±0.2		11.8±0.5
10.2±0.1		18.7±0.9	5.8±0.6		14.7±0.7
11.0±0.1	6.9±0.8	21.5±1.2	7.4±0.4		18.2±1.0
11.5±0.1	71.6±3.5	23.3±0.8	8.0±0.5	209.3±21.9	18.7±0.8
12.5±0.1	309.7±10.5	26.9±1.0	10.5±0.4	534.6±37.6	22.9±0.9
13.25±0.10	609.9±19.1	28.8±1.3	12.2±0.7	845.0±60.7	26.9±0.9
14.0±0.1	694.9±22.3	29.0±0.8	11.8±0.4	896.5±64.4	25.5±1.3
14.5±0.1	688.1±21.6	29.1±0.8	11.8±0.4	969.7±68.9	27.2±1.5
15.0±0.1	713.5±22.4	30.0±0.9	11.8±0.4	918.6±65.5	28.0±1.3

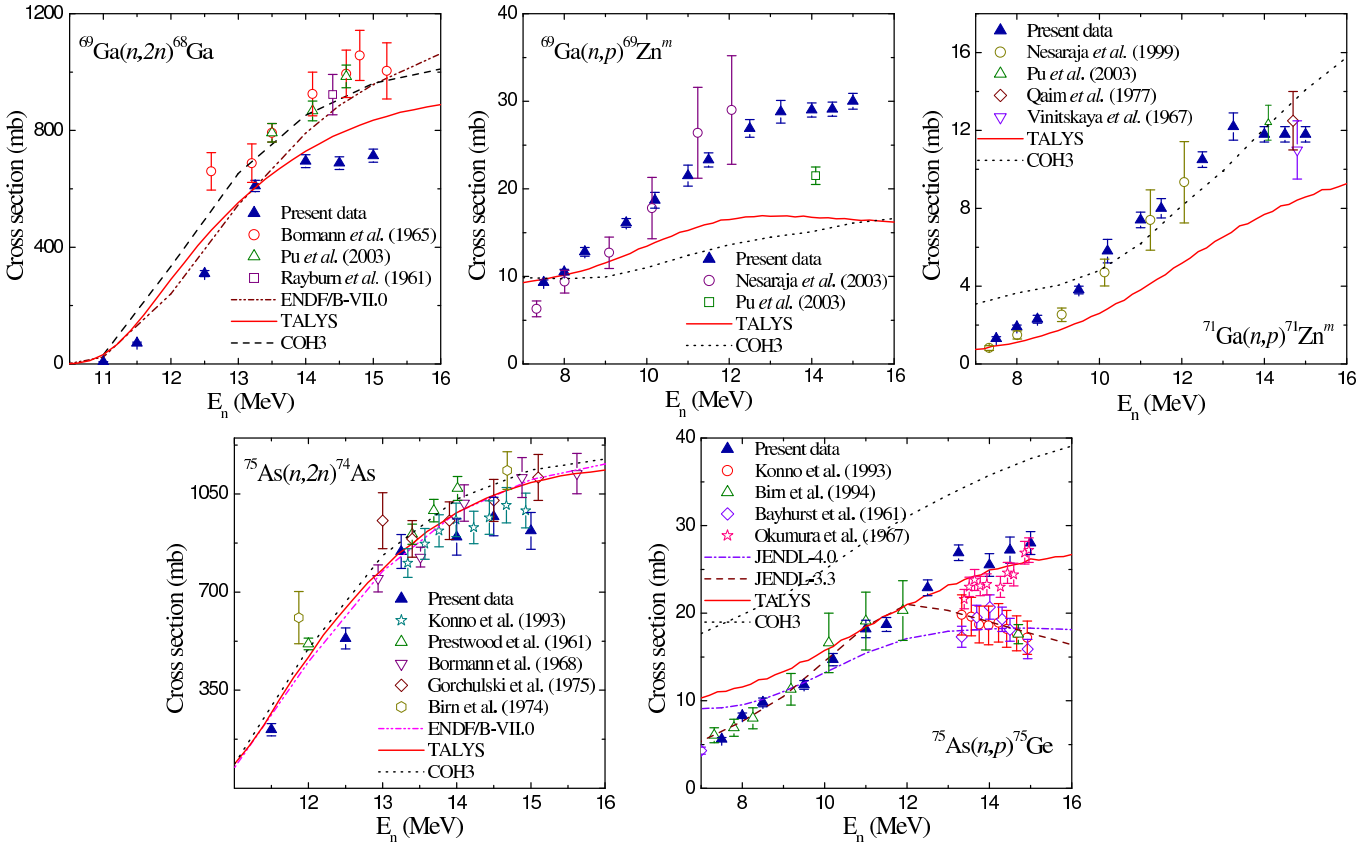

FIG. 5: (Color online). Reaction cross section as a function of incident neutron energy for the reactions studied in the present work. Each plot also includes theoretical calculations using statistical model codes as well as the latest evaluations and literature data.

The measured cross-section of the ^{75}As$(n,2n)^{74}$As reaction from the present work is lower than the available literature data at lower energies. At energies above 13 MeV the present measurements agree well with that of Konno *et al.* [5, 6], but those by Prestwood *et al.* [22], Grochulski *et al.* [23], and Birn *et al.* [4] are consistently higher than the present measurements over the entire energy range. The ENDF/B-VII.0 evaluations are in reasonable agreement with the present measurements apart from the 15 MeV data point. Interesting observations

are made for the ^{75}As$(n,p)^{75}$Ge reaction with respect to the literature data. The present measurements show a continuously increasing cross-section for this reaction in the chosen energy range from 7.5 to 15 MeV, as illustrated in Fig. 5. The measured cross-section agrees well with the data from Birn *et al.* [4] below 13 MeV. However, above 13 MeV, the literature data from Birn *et al.* [4], Konno *et al.* [5, 6], and Bayhurst *et al.* [24] show a decrease in the cross section while the present measurement and the results of Okumura *et al.* [7] show a continuous increase. The JENDL-3.3 evaluation has excellent overlap with the present measurements below 13 MeV, but follows the decreasing trend reported in most of the previous measurements at higher energies. The latest JENDL-4.0 [25], however, has poor agreement with the present data and with the results of Birn *et al.* [4] at lower energies, and it approximately agrees with the previous measurements in the 13-15 MeV region.

In the present work, the reaction channels ^{75}As(n,α) and ^{71}Ga(n,γ) led to the production of the same residual nucleus ^{72}Ga so that the measured cross-section could not be unambiguously ascribed to a particular channel.

B. Statistical Model Calculations with Default Parameters

The statistical-model calculations, based on the Hauser-Feshbach formalism, were carried out using two different codes, TALYS-1.2 [18] and COH3 [26]. The results of these calculations are plotted along with the experimental data in Fig. 5. Before we embark on discussing the results for the specific reactions, we mention the salient features of the said calculations.

Initially, the calculations using TALYS-1.2 (hereafter referred as TALYS) and COH3 were carried out using the default parameters of the codes and the results are plotted in Fig. 5. The optical model potential (OMP) parameters in the TALYS calculations are from the local and global parametrization of Koning and Delaroche [18]. It is noted that TALYS resorts to the global OMP parameter set in the absence of a local one and this was the case for the proton OMP used in the present calculations. However, for the neutron OMP, specific (local) parameter sets exist in the TALYS database for the Ga and As isotopes. The present measurements extend up to 15 MeV incident neutron energy and the preequilibrium processes are expected to assume significance at energies above 10 MeV. TALYS uses the exciton model based on numerical transition rates with energy dependent matrix element as the default choice for the preequilibrium reactions. As far as the level density input is concerned, the model introduced by Gilbert and Cameron [27] is adopted as the default option in TALYS. This model is a combination of the Constant Temperature Model (CTM) at lower energies and the Fermi Gas Model (FGM) at the higher energies. A matching temperature is computed within the program, below which the CTM is applied and beyond which the FGM becomes operational. For the γ-ray strength function, the Kopecky-Uhl generalized Lorentzian is used for the E1 transitions and the Brink-Axel Lorentzian is invoked [18] for all other transition types. A similar set of nuclear models is also used in COH3 [26] as the default choice. However, there are certain differences in the parametrizations used by the two codes, for instance, in the case of the preequilibrium models.

A common input file with all the aforesaid default options was used to calculate the ^{69}Ga$(n,2n)^{68}$Ga and the ^{69}Ga$(n,p)^{69}$Zn^m reaction cross sections. The results plotted in Fig. 5, indicate reasonable agreement with the experimental data for the ^{69}Ga$(n,2n)^{68}$Ga reaction. It is noteworthy that the calculated excitation function for the ^{69}Ga$(n,2n)$ reaction is closer to the present data compared to the existing literature values. However, for the much weaker ^{69}Ga$(n,p)^{69}$Zn^m reaction channel, the calculated cross section from TALYS and COH3 codes, with their default parameters, substantially underpredict the present measurements as well as the existing literature data by as much as a factor of two at the highest energies. At the lowest incident energies around 8 MeV, the calculated excitation function overlaps well with the data, but then assumes an unrealistically flat shape at higher energies. Similarly, for the ^{71}Ga$(n,p)^{71}$Zn^m reaction, there is a large discrepancy between the TALYS calculated excitation function with both the present and the literature data, especially for energies above 8 MeV. The COH3 calculated cross-sections for this reaction roughly agree with the measured values in the energy range 9-14 MeV. However, at lower energies around 8 MeV and above 14 MeV, COH3 overpredicts the ^{71}Ga$(n,p)^{71}$Zn^m cross sections, with respect to the present measurements.

The aforesaid discrepancies between the calculated and the measured cross-sections of the (n,p) channels can be addressed as follows. The (n,p) channel is a weak channel with only about 1% of the total reaction cross section. Thus the cross-section predictions for this channel are very sensitive to the small variations in the many parameters of the statistical model calculations. For instance, the proton OMP parameters are not well determined around the Coulomb barrier energies covered in the present measurements. The uncertainties in the OMP parameters would thus affect the cross-section predictions. Further, the (n,p) channel is known to have a significant preequilibrium contribution and the uncertainties in the parametrization of the preequilibrium models would significantly impact the results.

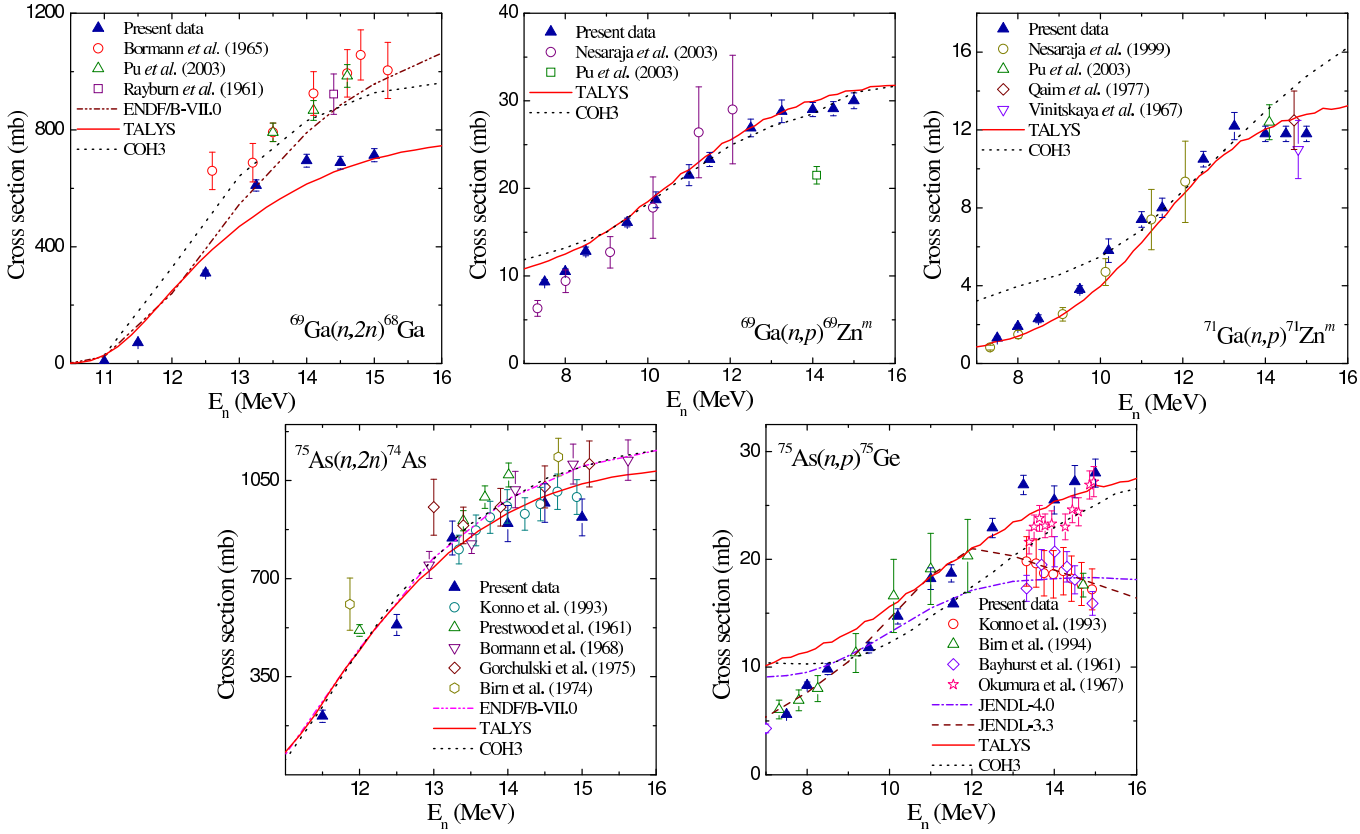

FIG. 6: (Color online). Plot similar to Fig. 5 except that the TALYS and the COH3 plots here were calculated by adjusting the level density parameters. Please refer to the text for individual parameter adjustments.

Similar features have been observed for the calculated cross sections of the $(n, 2n)$ and (n, p) reactions on ^{75}As. The calculated cross-sections for the ^{75}As$(n, 2n)$ reaction comply satisfactorily with the current data for all energies, except at 15 MeV where the present data point is lower (within uncertainties) compared to the previous measurements. For the (n, p) reaction channel, the TALYS results are in better agreement with the present measurements and the previous data, except for the near proton separation energies in ^{75}As(n, p) reaction. On the other hand, the COH3 results for the same reaction substantially overpredict the cross-section values for all energies. As in the case of ^{69,71}Ga(n, p) reactions, the discrepancy for the ^{75}As(n, p) channel too can be ascribed to the uncertainties pertaining to the statistical model parameters. This is corroborated by the observations of Shibata *et al.* [25] in JENDL-4.0 evaluations. It appears that the experimental excitation function for the ^{75}As(n, p) reaction near the threshold cannot be reproduced by the standard parametrization in the Hauser-Feshbach model codes. A possible solution is to replace the proton global optical model potential with a locally valid one for this mass region. However, such exercise needs to be justified by experimental endeavors aimed at obtaining better optical model potentials near the Coulomb barrier, although it would be experimentally challenging to distinguish the nuclear interactions from Coulomb scattering.

C. Statistical Model Calculations with Adjusted Parameters

In view of the large discrepancies between the measured excitation function and that calculated from the statistical model codes TALYS and COH3, using default parameters, for the ^{69}Ga$(n, p)^{69}$Zn^m, ^{71}Ga$(n, p)^{71}$Zn^m and, ^{75}As(n, p) reactions, the corresponding calculations were revisited with the objective of fitting the experimental data with an adjusted but physically relevant parameter set. The motivation for such adjustments is to identify the parameters that have a bigger impact on the calculations and to understand the physical justification for the adjustments. At the same time, it was also necessary to check on the impact of such adjustments on the calculated excitation function of the dominating $(n, 2n)$ channel. There are a large number of parameters involved in the statistical model calculations and it is an elaborate exercise to address each of them within the scope of the present work. The Optical Model Potential (OMP) and the level density parameters, however, are

TABLE IV: Default values and adjustments for the level density parameters in the statistical model calculations using TALYS and COH3

Reaction	Nucleus	Default Value			Adjustments in COH3			Adjustments in TALYS		
		g_ν	g_π	a	g_ν	g_π	a	g_ν	g_π	a
^{69}Ga$(n,2n)$, (n,p)	^{69}Zn	2.60	2.00	11.51		+30%	+10%			
	^{69}Ga	2.53	2.07	10.96				-30%		
	^{70}Ga	2.60	2.07	10.11				-20%	-10%	
^{71}Ga(n,p)	^{71}Zn	2.73	2.00	12.40			-10%	+30%		+20%
^{75}As$(n,2n)$, (n,p)	^{75}As	2.80	2.20	12.82	+3%	-15%	+20%	-15%	+30%	
	^{75}Ge	2.87	2.13	12.55			+10%			
	^{72}Ga	2.73	2.07	11.48			+20%			

of primary significance and were individually adjusted to fit the data acquired from the current measurements.

We first discuss the adjustments in the level density parameters and the results obtained therefrom. Phenomenological level densities are often expressed by the Gilbert-Cameron-type level density formula [27] or the back-shifted Fermi-gas formula [28]. As already discussed in the previous section, we apply here the Gilbert-Cameron-type (GC) formula, which includes the Fermi-gas model

$$\rho_G(E_x,J) = \frac{1}{12\sigma\sqrt{2}}\frac{\exp\left(2\sqrt{aU}\right)}{a^{1/4}U^{5/4}}\frac{2J+1}{2\sigma^2} \times \exp\left\{-\frac{(J+1/2)^2}{2\sigma^2}\right\}, \quad (3)$$

with,

$$U = E_x - \Delta, \quad (4)$$

at higher excitation energies, and the constant-temperature model

$$\rho_T(E_x,J) = \frac{1}{T}\exp\left(\frac{E_x-E_0}{T}\right)\frac{2J+1}{2\sigma^2} \times \exp\left\{-\frac{(J+1/2)^2}{2\sigma^2}\right\}, \quad (5)$$

at lower excitation energies, where a is the level density parameter, T is the nuclear temperature, E_0 is the energy shift and σ^2 is the spin-cutoff factor. Those two expressions are connected smoothly at a certain matching energy E_m, with the matching condition of $\rho_G = \rho_T$ and $d\rho_G/dE = d\rho_T/dE$ at $E = E_m$, so that T and E_0 are determined automatically when a and discrete level information are provided [29].

In addition, the single particle state density parameters, g_π and g_ν which respectively represents the spacing of the proton and the neutron single particle states near the Fermi energy, can also be adjusted to fit the experimental data. By default, $g_\pi = Z/15$, Z being the proton number and $g_\nu = N/15$, N being the neutron number. In the model calculations using TALYS and COH3 a, g_π and g_ν were independently adjusted with respect to the default values to fit the present data. However, owing to the difference in level density parametrizations used in the two codes, the magnitude of adjustments and the particular nuclei (compound or residual) adjusted were different in each.

The default values of the level density parameters and the adjustments adopted to fit the data, with TALYS as well as COH3, are recorded in Table IV. The adjustments are, for some cases, as high as 30% probably reflecting the less sensitive nature of the level density parameters to make an impact on the results of the statistical model calculations. The level density adjustments had to be applied to the residual nuclei of interest as well as, in specific cases, to the target and the first compound nucleus. The results of these calculations with adjusted level density parameters are illustrated in Fig. 6.

For the ^{69}Ga$(n,p)^{69}$Zn^m reaction, the calculated excitation functions with adjusted level densities are in excellent agreement with the data from the present measurements and the literature values. This is significantly improved from the poor overlap of the calculated excitation function with default parameters and the measured

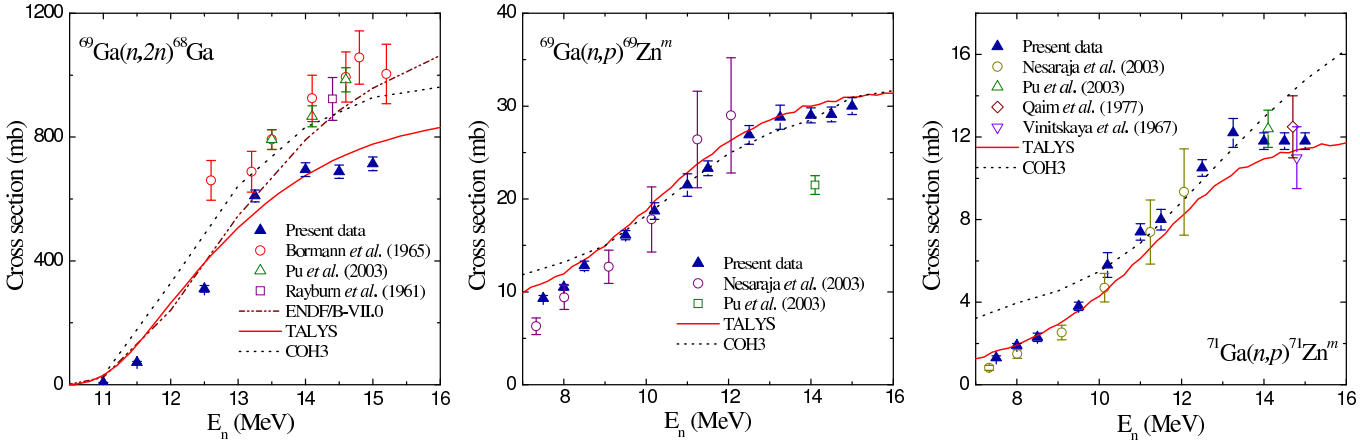

FIG. 7: (Color online). Plot similar to Fig. 6 except that the TALYS plots here were calculated by adjusting the OMP parameters. Please refer to the text for individual parameter adjustments. The COH3 plots are identical to those in Fig. 6. No significant improvement was found in the TALYS calculated cross sections of ^{75}As reactions, by OMP adjustments and thus these reactions have not been included in the figure.

cross sections, illustrated in Fig. 5. These calculations, with adjusted level density parameters in TALYS, affect the fitting of the dominant ^{69}Ga$(n, 2n)$ channel as well, observed from comparing Fig. 6 with Fig. 5. TALYS calculations with default parameters agree well with the ^{69}Ga$(n, 2n)$ cross-sections at the 13-14 MeV region, but overpredict the measured cross section around 15 MeV by about 20%. The same calculations with level density adjusted parameters shows excellent agreement with the present measurements around 15 MeV, but underestimates the cross section by about 20% in the 13-14 MeV region.

For the ^{71}Ga$(n, p)^{71}$Zn^m reaction, the calculated excitation functions with adjusted level densities have different agreement with the data in the cases of the TALYS and the COH3 calculations, as seen in Fig. 6. The level density adjusted calculations in TALYS, for this reaction, yield an excellent agreement with the current measurements and the literature data at all energies in the 7 to 15 MeV range. This is distinctly improved from the TALYS calculated excitation function of Fig. 5, carried out with default parameters, that largely underpredicts the measurements at all energies above 9 MeV. However, COH3 calculations with level density adjustments for this reaction remain similar to the default calculations, with an excitation function that agrees with the data in the energy range from 10 to 13 MeV, but overpredicts the measured cross sections in the 7 to 10 MeV and above 14 MeV region, as illustrated in Fig. 6.

For the reactions on ^{75}As, the parameter adjustments were more complicated in order to obtain a reasonable fit for all the reaction channels. The resulting fit for the ^{75}As(n, p) and $(n, 2n)$ reaction cross-sections is illustrated in Fig. 6. As far as the TALYS code is concerned, the difference from the default calculations is marginal for the ^{75}As reactions. The overlap of the calculated excitation function with the measured cross sections remain satisfactory for the ^{75}As$(n, 2n)$ reaction, while the level density adjustments could not compensate the overprediction of the code for the ^{75}As(n, p) cross section in the energy range from 7 to 10 MeV. The COH3 calculated excitation function for the ^{75}As$(n, 2n)$ reaction, with adjusted level densities, also remains largely similar to the default calculations. However, the calculated excitation function of the ^{75}As(n, p) channel, using level density adjustments, is in substantially better agreement with the present data, compared to the calculations with default parameters. It is noteworthy to stress that no adjustment in the realistic limits of the statistical model parameters could reproduce the decreasing trend of the ^{75}As(n, p) cross section beyond 13 MeV while still fitting the increasing values in the 7 to 13 MeV range. Such exercise can be cited to indicate the validity of the present measurements, partly supported by the results from Okumura *et al.* [7] that show the same increasing trend above 13 MeV, but differs in the cross-section values with respect to the current work.

The large amount of adjustments in the level density parameters, required to fit the data, most likely indicates the less sensitive nature of these parameters in the statistical model calculations. An alternate procedure was adopted for fitting the data from the present work, by tuning the OMP parameters only in the TALYS code that allows for such adjustments. It is understood that OMP parameters are more fundamental in the statistical calculations and might not be tuned for fitting any specific reaction channel from a particular measurement. Nevertheless, as already mentioned at the onset of this section, the exercise was motivated by an impetus to investigate the sensitivity of different

parameters to the results of the statistical calculations. Further justification to address the OMP parameters in particular will be discussed in due course.

To fit the ^{69}Ga$(n,p)^{69}$Zn^m along with ^{69}Ga$(n,2n)^{68}$Ga data in the TALYS code, the diffuseness parameter of the volume-central potential for the proton OMP was reduced by 10%. As already mentioned before, in the absence of a local parameter set for the OMP, TALYS uses the global parametrization of Koning and Delaroche [18] by default, as is the case in the present calculations for ^{69,71}Ga and ^{75}As, which do not have a nucleus specific local parameter set for the proton OMP. According to the global parametrization, the diffuseness parameter of the volume-central part in the proton OMP is given by,

$$a_V = 0.6778 - 1.487 \times 10^{-4} A \tag{6}$$

where A is the mass number for the nucleus. Further, the preequilibrium model, for the ^{69}Ga reactions only, was changed from the default exciton to the multi-step direct / compound model. Such adjustments in the preequilibrium model and the diffuseness parameter led to an excellent agreement with the experimental data, especially for the weaker (n,p) channel that was significantly underpredicted in the default calculations. The adjustments also led to a reasonably satisfactory fitting of the ^{69}Ga$(n,2n)^{68}$Ga data from the present measurements.

Next, in the TALYS parameter set for fitting the ^{71}Ga$(n,p)^{71}$Zn^m reaction, the radius and the diffuseness parameters of the volume-central part of the proton OMP were each incremented by 10% with respect to the default value. The global diffuseness parameter has been described in the previous equation, while the global radius parameter for the volume-central part of the proton OMP is given by,

$$r_V = 1.3039 - 0.4054 A^{-1/3} \tag{7}$$

The resulting excitation function for the ^{71}Ga$(n,p)^{71}$Zn^m reaction is in satisfactory agreement with the present measurements compared to the under represented cross-sections in the default calculations.

For the ^{75}As reaction cross-sections, no significant improvement was observed by OMP adjustments compared to the previous fitting with default parameters or by tuning the level density parameters. Thus, no plot for the ^{75}As reactions have been explicitly included in Fig. 6.

It is difficult to justify the aforesaid adjustments within the purview of the current work. As already noted, one possible explanation could be based on the fact that the (n,p) reaction channels are much weaker than the $(n,2n)$ channels. Further, at energies around the Coulomb barrier, the global OMP parameters, at least for the protons, are not well established and consequently a 10% adjustment can be accepted as legitimate. The requirement for a different preequilibrium model to fit the ^{69}Ga(n,p) data is even more obscure. It requires to be pursued if this indicates a dependence of the preequilibrium phenomena and thus the corresponding modeling, on the structural aspects of the nucleus, or if it is simply a consequence of the preequilibrium parametrization in the TALYS code.

It is thus observed that while the calculated excitation functions for the dominant $(n,2n)$ reaction channel are not significantly affected by moderate parameter adjustments, the impact on the weaker (n,p) channel is large. Further, the calculations appear more sensitive to the changes in OMP parameters than the level density adjustments carried out in the present work. Experiments and phenomenological pursuits are still in requirement for credible parametrizations, especially in the charged particle OMP, that would accurately describe the weaker channels in conjunction with the dominant ones.

V. SUMMARY AND CONCLUSIONS

Cross-section measurements were carried out for neutron induced reactions on Ga and As isotopes in the energy range from 7.5 to 15 MeV. Monoenergetic neutron beam, pure samples, and high resolution HPGe detectors were used to restrict the uncertainties in the measurements. The cross-section results were compared with the literature data and found largely to be in satisfactory compliance. Statistical-model calculations were carried out based on the Hauser-Feshbach formalism using different codes with default and adjusted parameter sets. The agreement of the calculated excitation functions with the experimental data vary with different reactions and parameter adjustments.

This work has contributed to the understanding of the neutron induced reactions on the individual Ga and As isotopes, that can be extrapolated to interpreting the characteristics of the GaAs semiconductor in high radiation environments. The said understanding can be applied to the issues pertaining to the national security viz., nuclear forensics and the stockpile stewardship program.

VI. ACKNOWLEDGEMENTS

The authors are grateful to Dr. C. Kalbach Walker and Dr. A.J. Koning for helpful discussions on statistical-model calculations and the TALYS code. This work is supported in part by the National Nuclear Security Administration (NNSA) under the Stewardship Science Academic Alliance Program through the US Department of Energy grant DE-PS52-08NA28920, DE-FG52-06NA26155 and by Los Alamos National Laboratory (W-7405-ENG-36).

[1] H. Xu, A. Amann, E. Schöll, and S. W. Teitsworth, Phys. Rev. B **79**, 245318 (2009).
[2] C. Nesaraja, S. Sudar, and S. Qaim, Phys. Rev. C **68**, 024603 (2003).
[3] C. Nesaraja, K. Linse, S. Spellerberg, S. Sudar, S. Suhaimi, and S. Qaim, Radiocim. Acta. **86**, 1 (1999).
[4] I. Birn and S. Qaim, Nucl. Sci. Eng. **116**, 125 (1994).
[5] C. Konno, Y. Ikeda, K. Oishi, K. Kawade, H. Yamamoto, and H. Maekawa, JAEARI Rep. **No. 1329** (1993).
[6] C. Konno, Y. Ikeda, K. Oishi, K. Kawade, H. Yamamoto, and H. Maekawa, JAEARI Rep. **No. 1312** (1988).
[7] S. Okumura, Nucl. Phys. A **93**, 74 (1967).
[8] Z. Pu, J. Yang, and X. Kong, App. Rad. Iso. **58**, 723 (2003).
[9] M. Bormann, E. Fretwurst, P. Schehka, G. Wrege, H. Büttner, A. Lindner, and H. Meldner, Nucl. Phys. **63**, 438 (1965).
[10] A. S. Crowell, *Priv. comm.* (2009).
[11] URL `homepage.univie.ac.at/manfred.drosg/drosg2000.htm`.
[12] J. Theurkauf, S. Esser, S. Krink, M. Luig, N. Nicolay, O. Stuch, and H. Wolters, *Tv program*.
[13] URL `www.nndc.bnl.gov/nudat2/`.
[14] P. Reimer, Ph.D. thesis, No. 3980, Forschungszentrum Jülich, University of Cologne (2002).
[15] J. Martínez-Rico, Tech. Rep. INDC(NDS)-285 Distr. G, International Nuclear Data Committee (1993).
[16] H. Condé, Tech. Rep. NEANDC-311"U" INDC(SEC)-101, Nuclear Energy Agency (1992).
[17] A. P. Tonchev, C. T. Angell, M. Boswell, A. S. Crowell, B. Fallin, S. Hammond, C. R. Howell, A. Hutcheson, H. J. Karwowski, J. H. Kelley, et al., Phys. Rev. C **77**, 054610 (2008).
[18] A. Koning, S. Hilaire, and M. Duejvestijin, in *Proceedings of the International Conference on Nuclear Data for Science and Technology* (Nice, France, 2008), p. 211.
[19] L. A. Rayburn, Phys. Rev. **122**, 168 (1961).
[20] N. Molla and S. Qaim, Nucl. Phys. A **283**, 269 (1977).
[21] G. Vinitskaya, V. Levkovskiy, V. Sokol'sky, and I. Kazachevskiy, Yad. Fiz. **5**, 1175 (1967).
[22] R. Prestwood and B. Bayhurst, Phys. Rev. **121**, 1438 (1961).
[23] W. Grochulski, S. El-Konsol, and A. Marcinkowski, Act. Phys. Pol. B **6**, 139 (1975).
[24] B. Bayhurst and R. Prestwood, Jour. Inorg. Nucl. Chem. **23**, 173 (1961).
[25] K. Shibata, G. Chiba, A. Ichhihara, and S. Kunieda, Jour. Nucl. Sci. Tech. **47**, 40 (2010).
[26] T. Kawano, *Priv. comm.* (2010).
[27] A. Gilbert and A. Cameron, Can. Jour. Phys. **43**, 1446 (1965).
[28] W. Dilg, W. Schantl, H. Vonach, and M. Uhl, Nucl. Phys. A **217**, 269 (1973).
[29] T. Kawano, S. Chiba, and H. Koura, Jour. Nucl. Sci. Tech. **43**, 1 (2006).